Search for massive neutrinos in the decay π→eν

M. Aoki, M. Blecher, D. A. Bryman, S. Chen, M. Ding, L. Doria, P. Gumplinger, C. Hurst, A. Hussein, Y. Igarashi, N. Ito, S. H. Kettell, L. Kurchaninov, L. Littenberg, C. Malbrunot, T. Numao, R. Poutissou, A. Sher, T. Sullivan, D. Vavilov, K. Yamada, and M. Yoshida (PIENU Collaboration)

Phys. Rev. D **84**, 052002 — Published 6 September 2011

DOI: 10.1103/PhysRevD.84.052002

Search for Massive Neutrinos in the Decay $\pi \to e\nu$

M. Aoki[1], M. Blecher[2], D.A. Bryman[3], S. Chen[4], M. Ding[4], L. Doria[5], P. Gumplinger[5], C. Hurst[3], A. Hussein[6], Y. Igarashi[7], N. Ito[1], S.H. Kettell[8], L. Kurchaninov[5], L. Littenberg[8], C. Malbrunot[3], T. Numao[5], R. Poutissou[5], A. Sher[5], T. Sullivan[3], D. Vavilov[5], K. Yamada[1], M. Yoshida[1]
(PIENU Collaboration)
[1] *Physics Department, Osaka University, Toyonaka, Osaka, 560-0043, Japan*
[2] *Virginia Tech., Blacksburg, VA, 24061, USA*
[3] *Department of Physics and Astronomy, University of British Columbia, Vancouver, B.C., V6T 1Z1, Canada*
[4] *Department of Engineering Physics, Tsinghua University, Beijing, 100084, China*
[5] *TRIUMF, 4004 Wesbrook Mall, Vancouver, B.C., V6T 2A3, Canada*
[6] *University of Northern British Columbia, Prince George, B.C., V2N 4Z9, Canada*
[7] *KEK, 1-1 Oho, Tsukuba-shi, Ibaragi, Japan*
[8] *Brookhaven National Laboratory, Upton, NY, 11973-5000, USA*

Evidence of massive neutrinos in the $\pi^+ \to e^+\nu$ decay spectrum was sought with the background $\pi^+ \to \mu^+ \to e^+$ decay chain highly suppressed. Upper limits (90 % C.L.) on the neutrino mixing matrix element $|U_{ei}|^2$ in the neutrino mass region 60–129 MeV/c^2 were set at the level of 10^{-8}.

PACS numbers: 13.20.Cz, 14.60.St, 12.15.Ff

I. INTRODUCTION

A natural extension of the Standard Model (SM) incorporating neutrino mass and possibly explaining the origin of dark matter involves the inclusion of sterile neutrinos mixing with the ordinary neutrinos [1]. The weak eigenstates ν_{χ_k} of such neutrinos are related to the mass eigenstates ν_i by a unitary matrix, $\nu_\ell = \Sigma_{i=1}^{3+k} U_{\ell i}\nu_i$, where $\ell = e, \mu, \tau, \chi_1, \chi_2 \cdots \chi_k$. An example of a sterile neutrino model is the Neutrino Minimal Standard Model that adds to the SM three massive gauge-singlet fermions (sterile neutrinos) [2]. In the context of this model, a search for extra peaks in the $\pi^+ \to e^+\nu$ decay spectrum is sensitive to sterile neutrinos depending on the mass hierarchy structure and choice of parameters [3]. However, the result of the search is also applicable to other types of neutrinos [4].

The decay $\pi^+ \to e^+\nu$ ($E_{e^+} = 69.8$ MeV) with a branching ratio of $R = (1.230 \pm 0.004) \times 10^{-4}$ [5–7] is helicity-suppressed by $(m_e/m_\mu)^2$ in the SM. The relaxation of this condition for massive neutrinos facilitates the search for extra peaks in the lower positron energy region. Previous results [8] at the level of $|U_{ei}|^2 < 10^{-7}$ in the neutrino mass region of 70–130 MeV/c^2 were limited by the presence of unsuppressed $\mu^+ \to e^+\nu\overline{\nu}$ decay background ($E_{e^+} = 0.5 - 52.8$ MeV) originating from decay-in-flight of pions [5]. The TRIUMF PIENU experiment [9] aiming at a more precise measurement of the branching ratio R was designed to further reduce this background.

In this paper, we present results of the search for low-energy peaks in the background-suppressed spectrum of $\pi^+ \to e^+\nu$ decays at rest.

II. EXPERIMENT

The extension of the TRIUMF M13 beam line [10], which suppressed positrons in the beam to < 2 % of pions, delivered a 75±1 MeV/c pion beam to the experiment. Figure 1 shows a schematic view of the detector. The π^+ beam was degraded by two thin plastic scintillators B1 and B2 (6 mm and 3 mm thick, respectively) and stopped in an 8-mm thick active target (B3) at a rate of 5×10^4 π^+/s.

In order to obtain a large solid angle for e^+ detection from the decay $\pi^+ \to e^+\nu$ while reducing variations in material along the positron path, the primary calorimeter was placed on the beam axis. It consisted of two plastic scintillators (3-mm thick T1 and 6-mm thick T2) for positron identification and a 48-cm (dia.) × 48-cm (length) single-crystal NaI(Tℓ) detector [11] viewed by 19 photo-tubes. Two rings of 97 pure CsI crystals [12] (9 radiation length radially) surrounded the NaI(Tℓ) crystal to reduce leakage of the electromagnetic shower produced by a positron. The observed energy response of the NaI(Tℓ) detector to positrons from $\pi^+ \to e^+\nu(\gamma)$ decays included a peak at 70 MeV and a low-energy tail distribution.

Pion tracking was provided by wire chambers (WC1 and WC2) each with three planes (oriented at 0°, ±60°)

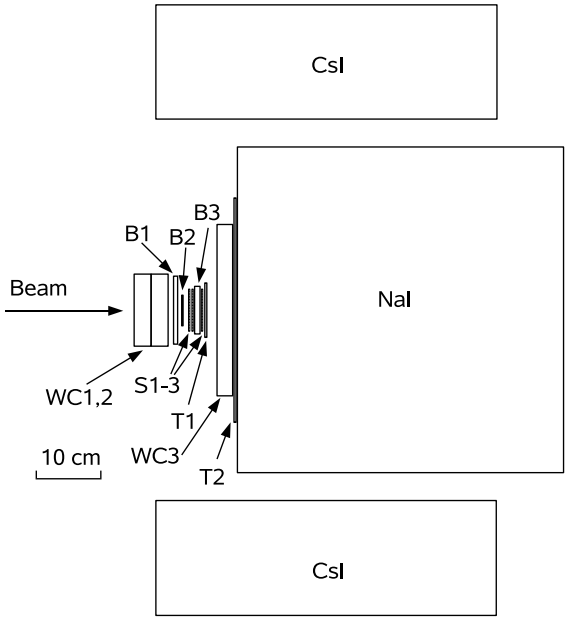

FIG. 1: PIENU Detector (see text).

at the exit of the beam line, and four planes of 0.3-mm thick X and Y Si-strip counters S1X/Y and S2X/Y located immediately upstream of the B3 counter. Positron tracking came from one set of X and Y Si-strip counters (S3X and S3Y) immediately downstream of the B3 counter, and three layers of wire chambers (WC3) in front of the NaI(Tℓ) crystal.

A coincidence of beam counters, B1, B2 and B3, with a high B1 threshold defined the pion signal, and a coincidence of positron counters, T1 and T2, defined the decay-positron signal. A coincidence of pion and positron signals with a time window of –300 ns to 500 ns was the basis of the main trigger logic. This was prescaled by a factor of 16 to form an unbiased trigger (Prescaled trigger), and the early time window (2–40 ns) provided another trigger (Early trigger) that contained most of $\pi^+ \to e^+\nu$ decays. Beam positrons for detector calibration were accumulated by a separate trigger that required a low pulse height in the B1 counter. A typical trigger rate was 600 Hz, of which 240 Hz was for Prescaled, 160 Hz for Early, and 5 Hz for Beam positron.

The pulse shapes from the plastic counters, the CsI crystals and Si-strip detectors, and the NaI(Tℓ) crystal were digitized at 500 MHz [13], 60 MHz, and 30 MHz, respectively.

III. ANALYSIS

A. Event selection

The charge and time of each pulse were first extracted from the waveform. Energy calibration of each detector was based on the energy loss of minimum ionizing particles (75 MeV/c positrons in the beam) for plastic and Si-strip counters, and 70 MeV positrons from $\pi^+ \to e^+\nu$ decays for the NaI(Tℓ) signals. Gain instability was corrected on a run-by-run basis (typically, every ten minutes).

Events originating from stopped pions were selected based on their energy losses in B1, B2, S1X/Y and S2X/Y, and the time-of-flight with respect to the primary-proton beam burst (or the phase of the cyclotron Radio Frequency). Events caused by beam positrons and muons were negligible after the cuts. Any events with extra activity in the beam counters including WC1 and WC2 were rejected. About 40 % of events survived the cuts.

An energy-loss cut based on the minimum energy-loss in T1, T2, S3X and S3Y was used to select decay-positrons. The cut reduced beam muons directly hitting those counters and protons coming from pion-nucleus reactions to a negligible level. A fiducial cut, requiring the hit position at WC3 to be within 8 cm from the beam axis, was imposed to reduce the low energy tail of the $\pi^+ \to e^+\nu$ peak due to shower leakage from the NaI(Tℓ) crystal. The low energy tail was further reduced by rejecting events with energy above 6 MeV in the CsI crystals.

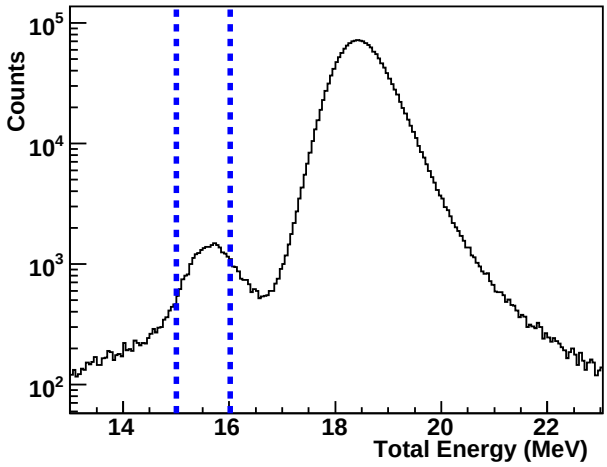

FIG. 2: Total energy in the beam counters. The peaks at 15.6 and 18.5 MeV are from $\pi^+ \to e^+\nu$ and $\pi^+ \to \mu^+ \to e^+$ decays, respectively. The selected region is between the vertical dashed lines.

In order to enhance the small $\pi^+ \to e^+\nu$ decay signal, the $\pi^+ \to \mu^+ \to e^+$ ($\pi^+ \to \mu^+\nu$ decay followed by $\mu^+ \to e^+\nu\overline{\nu}$ decay) background was suppressed using timing cuts to take advantage of the lifetime difference between pions and muons ($\tau_\pi = 26$ns and $\tau_\mu = 2197$ns). The time window selected was 2–33 ns following the pion stop time. Since the decay $\pi^+ \to e^+\nu$ involves only two charged particles while the decay $\pi^+ \to \mu^+ \to e^+$ has three charged particles with an extra kinetic energy of 4.1 MeV deposit from the $\pi^+ \to \mu^+\nu$ decay in B3, pulse

shape discrimination based on the likelihood for two and three pulses, and the total energy in the beam counters were also very effective in $\pi^+ \to \mu^+ \to e^+$ background suppression. In Figure 2, a spectrum of total energies in B1, B2, B3, S1X/Y and S2X/Y integrated over a time window of 100 ns is shown. The peaks at 15.6 and 18.5 MeV are from $\pi^+ \to e^+\nu$ and $\pi^+ \to \mu^+ \to e^+$ decays, respectively. (The energy separation between the two peaks is smaller than 4.1 MeV because of saturation effects in the plastic scintillator.) The vertical dashed lines indicate the cut positions. The ratio of the low energy events ($E_{e^+} < 54$ MeV, including the $\pi^+ \to e^+\nu$ tail) and the $\pi^+ \to e^+\nu$ peak ($E_{e^+} > 54$ MeV) was 0.2, consistent with that obtained in the previous TRIUMF experiment [8] (before the optimization process described below). At this stage, the major low-energy background in the background-suppressed spectrum came from decay-in-flight (DIF) of pions near the B3 counter, in which the muon from the $\pi^+ \to \mu^+\nu$ decay stopped in B3 and deposited the same kinetic energy as the initial pion [5].

The tracking detectors, S1X/Y and S2X/Y, allowed detection of a kink in the pion track when DIF happened upstream of the B3 counter. For the remaining events, the "pion" direction near B3 with respect to the beam direction is plotted in Fig. 3 for the regions $E_{e^+} > 54$ MeV (mostly $\pi^+ \to e^+\nu$) and $E_{e^+} < 32$ MeV (mostly pion DIF events with a negligible $\pi^+ \to e^+\nu$ tail contribution) by thin and thick lines, respectively. The background was suppressed by another factor of two by requiring the kink angle to be $< 14°$.

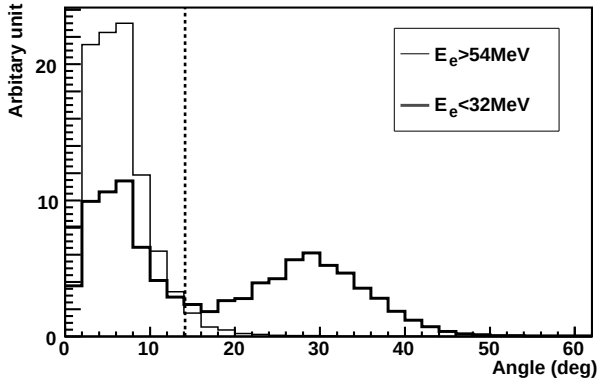

FIG. 3: Kink angles for events $E > 54$ MeV (thin) and $E < 32$ MeV (thick). The vertical dotted line at 14° indicates the cut position.

Also, consistency tests of the "pion" and positron tracks based on the closest approach of the two tracks in B3 provided an extra handle for suppressing the pion DIF events. An additional suppression factor of three was obtained with a loss of statistics of 30 %.

The cuts were optimized by minimizing the value $S = \sqrt{N_{<54\mathrm{MeV}}}/N_{>54\mathrm{MeV}}$, where $N_{<54\mathrm{MeV}}$ and $N_{>54\mathrm{MeV}}$ are the numbers of events below and above 54 MeV in the positron energy spectrum, respectively. The final background (including the low-energy tail of the $\pi^+ \to e^+\nu$ peak) to peak ratio was $N_{<54\mathrm{MeV}}/N_{>54\mathrm{MeV}} = 0.068$ with $N_{>54\mathrm{MeV}} = 4.8 \times 10^5$. The positron energy spectrum is shown as "No cut" in Fig. 4.

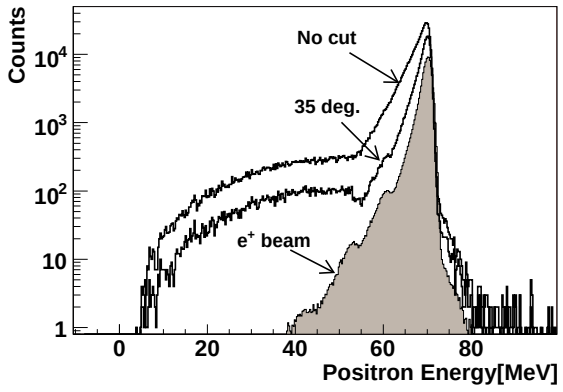

FIG. 4: Positron spectra with (35°) and without (No cut) angle cuts together with the positron beam spectrum shifted by 2.5 MeV (shaded).

B. Spectra with angle cut

There was a strong correlation between the emission angles of the decay positrons and the amount of the low energy tail due to shower leakage. As shown in Fig.4, the peak resolution was also improved by 10 % with the positron angle cut at 35° with respect to the beam axis ($\sigma = 0.8$ % (RMS for the high-energy side) at 70 MeV with the 35° cut). This cut also contributed to a better peak-to-background ratio. However, tighter cuts on the positron emission angle worsened the S value. Using spectra with the angle cut was effective only above 47 MeV where the impact of the resolution was higher.

There was a shoulder in the positron spectrum approximately at 60 MeV that was enhanced with the angle cut. Similar structures observed in the spectrum of the 75-MeV/c beam positron shown by the shaded histogram in Fig.4 were discussed in Ref.[14]. (To compensate for the difference in the initial energies and the additional energy losses of the beam positrons in B1, B2 and B3, the beam-positron spectrum was shifted by 2.5 MeV to line up with the $\pi^+ \to e^+\nu$ peak.) The bumps (or shoulders) at 60 MeV and 53 MeV in the beam positron spectrum correspond to the primary peak energy minus one and two neutron separation energies in ^{127}I, respectively; the loss of the energy observed in the NaI(Tℓ) crystal is due to low-energy neutrons produced in photo-nuclear reactions escaping from the crystal. Since this 60 MeV shoulder in the suppressed spectrum is consistent with the response function of the NaI(Tℓ) crystal [14], it was treated as background in the present study.

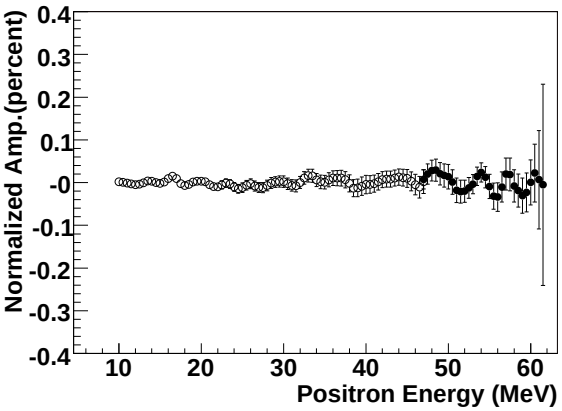

FIG. 5: Normalized amplitudes (%) of potential peaks for the no-cut spectrum (open circles) and for the 35° spectrum (closed circles).

C. Fitting

The search for extra peaks was conducted with 0.5 MeV steps in the positron energy regions, $E_{e^+} = 10 - 47$ MeV for the spectrum without the angle cut and $E_{e^+} = 47 - 60$ MeV with the 35° cut to take advantage of improved energy resolution obtained using the cut. The entire spectrum (9-50 MeV for the no-cut data and 9-62 MeV for the data with the 35° cut) was fitted to a background function (described below) plus a possible peak.

In order to minimize the effects of the bumps in the response function, the beam positron spectrum was subtracted from the spectra before the fitting search. The normalization was done in such a way that the 60 MeV peak amplitude in the fit of the spectrum with the 35° cut was zero.

The amplitude of the $\pi^+ \to \mu^+ \to e^+$ background, for which the spectrum was obtained with a late time window (150–500 ns), was a free parameter in the fit.

The positrons from DIF muons emitted promptly following $\pi^+ \to \mu^+\nu$ decays (about one third of the total $\pi^+ \to \mu^+ \to e^+$ background) decreased with the pion decay time, and the $\pi^+ \to \mu^+ \to e^+$ spectrum obtained from the late time window did not include this component. The muon-DIF spectrum was obtained by applying a Lorentz transformation for the muon kinetic energies 3.3–4.1 MeV to the $\pi^+ \to \mu^+ \to e^+$ spectrum with acceptance corrections (described in the next section) and muon polarization effects. The resulting muon-DIF spectrum had a broad bump around 30–40 MeV, extending near the $\pi^+ \to e^+\nu$ peak. The amplitude of this component was a free parameter of the fit.

In order to accommodate a slowly changing spectrum mismatch and unspecified background, the amplitude and the decay constant of an exponential function and an additional constant term were free parameters of the fit.

The template peak spectrum for each peak energy was obtained by applying the same cuts used in the data analysis to the positrons which were generated by a Monte Carlo (MC) simulation in the B3 counter with the observed pion stopping distribution. Measurements using positron beams at various entrance angles and energies into the NaI(Tℓ) crystal confirmed the validity of the MC line shapes including the effects of CsI vetoing. Agreements between the data and MC in the peak shape were within 10 %.

Figure 5 shows normalized amplitudes with errors (in standard deviation) of fitted peaks for the spectra without the angle cut (open circles) and with the 35° angle cut (closed circles). The χ^2/DOF's were 0.97 without the angle cut and 1.00 with the angle cut for the fits without the extra peak. The residual spectra of the fits were examined to be free of structures beyond statistical fluctuations, confirming the "perfect" χ^2/DOF's. The most significant positive deviation in Fig. 5 was 2.0 σ at $E_{e^+} = 16.5$ MeV (122 MeV/c^2 in neutrino mass).

D. Acceptance

Since the low-energy peak amplitudes obtained were normalized to that of the 70 MeV peak, most acceptance effects canceled to first order, especially those related to the pion definition cuts. There were, however, some energy-dependent effects in the cuts to be corrected for. The acceptances were estimated based on MC calculations. The consistency was tested to be within 3 % by comparing the MC and experimental $\pi^+ \to \mu^+ \to e^+$ spectra in the 10–50 MeV region with and without the background suppression cuts.

The fiducial cut increased the relative acceptance for 10 MeV positrons by 5 % (for no angle cut) with respect to 70 MeV positrons due to multiple scattering effects. Energy leakage into the CsI crystals for higher positron energy resulting in rejection of events also increased the relative acceptance of 10 MeV positrons by 15 %.

Because of larger scattering cross sections at lower energy, even within a small path length in B3 (3 mm in depth), lower energy positrons tended to have a larger total energy deposit in the target, thus lower energy events looked more like $\pi^+ \to \mu^+ \to e^+$ decays, causing a 10 % loss (no angle-cut data) in efficiency due to the total energy cut. The largest energy-dependent effect was in the vertex consistency requirement for pion and positron tracks, which reduced the acceptance of low energy positrons by 60 %. The combined acceptances for 10 MeV positrons with respect to 70 MeV positrons were 45 % (35° data) and 42 % (no cut).

IV. RESULTS

No significant peaks above statistical fluctuations were observed. After correcting for the acceptance and the helicity-suppression and phase-space terms [4], the amplitudes and associated errors were converted to 90 % C.L. upper limits on $|U_{ei}|^2$, assuming a Gaussian probability distribution with a constraint that the physical region of a peak area be positive. Figure 6 shows the combined results for the fits with the 35° angle cut (below 80 MeV/c^2 in neutrino mass), and without the angle cut (above 80 MeV/c^2). The region below 60 MeV/c^2 ($E_{e^+} > 57$ MeV) was excluded in the plot because of the strong bias caused by the background subtraction procedure. For comparison, the 90 % C.L. upper limits obtained in Ref. [8] are also plotted by a dashed curve.

The present experiment improved the upper limits on the neutrino mixing matrix element $|U_{ei}|^2$ by a factor of up to four in the mass region 90–110 MeV/c^2. However, the improvement in the regions below 90 MeV/c^2 and above 110 MeV/c^2 were not significant. In the previous experiment, the parameters for the background spectrum were determined from the spectrum in the search and fixed in the peak-search fit. This may have caused some bias, especially in the region below 90 MeV/c^2, where changes in the spectrum occurred with large statistics. The limited improvement for the present anaysis in the region above 110 MeV/c^2 may be due to the absence of energy dependent acceptance corrections in the analysis of the previous experiment though the variation was smaller; also the positron peak template for each energy was scaled from the $\pi^+ \to e^+\nu$ spectrum with the same low-energy tail fraction, while in the present experiment the templates were generated by MC calculations which were confirmed by data.

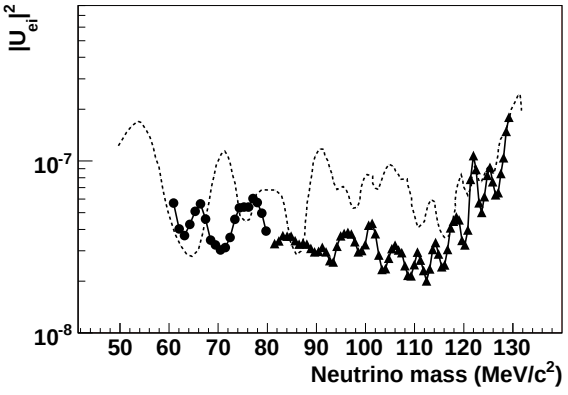

FIG. 6: Combined 90 % C.L. upper limits obtained from the 35° spectrum (circles) and no-cut spectrum (triangles) together with the previous limits (dashed line) [8].

V. CONCLUSIONS

The present experiment improved the upper limits on the neutrino mixing matrix element $|U_{ei}|^2$ by a factor of up to four in the mass region 68–129 MeV/c^2.

Acknowledgments

This work was supported by the Natural Science and Engineering Research Council and TRIUMF through a contribution from the National Research Council of Canada, and by Research Fund for the Doctoral Program of Higher Education of China, and partially supported by KAKENHI (21340059) in Japan, One of the authors (M.B.) has been supported by US National Science Foundation Grant Phy-0553611. We are grateful to Brookhaven National Laboratory for the loan of the crystals, and to the TRIUMF detector, electronics and DAQ groups for their engineering and technical support.

[1] A. Kusenko, Phys. Rep. 481, 1 (2009) and references therein.
[2] A. Boyarsky, O. Ruchayskiy and M. Shaposhnikov, Ann. Rev. Nucl. Part. Sci. 59 (2009) 191-214.
[3] T. Asaka, S. Eijima and H. Ishida, J. High Energy Phys. 1104, 011 (2011).
[4] R.E. Shrock, Phys. Rev. D24, 1232 (1981).
[5] D.I. Britton *et al.*, Phys. Rev. Lett. 68, 3000 (1992); and

D.I. Britton *et al.*, Phys. Rev. D49, 28 (1994).
[6] G. Czapek *et al.*, Phys. Rev. Lett. 70, 17 (1993).
[7] K. Nakamura *et al.* (Particle Data Group), J. Phys. G37, 075021 (2010).
[8] D.I. Britton *et al.*, Phys. Rev. D46, R885 (1992).
[9] PIENU experiment, TRIUMF Proposal S1072, (2005).
[10] A. Aguilar-Arevalo *et al.*, Nucl. Instrum. Method A609, 102 (2009).
[11] G. Blanpied *et al.*, Phys. Rev. Lett. **76**, 1023 (1996).
[12] I-H. Chiang *et al.*, IEEE Trans. Nucl. Sci. 42, 394 (1995).
[13] K. Yamada *et al.*, IEEE Trans. Nucl. Sci. 54, 1222 (2007).
[14] A. Aguilar-Arevalo *et al.*, Nucl. Instrum. Method A621, 188 (2010).